Hindawi
Advances in Civil Engineering
Volume 2020, Article ID 6621333, 8 pages
https://doi.org/10.1155/2020/6621333

Research Article

FE Modeling for Bolted Wood Connection Using a Porous Constitutive Model

Huazhang Zhou[1,2] **and Xiaoqiang Zhou**[2]

[1]*Key Lab of Structures Dynamic Behaviour and Control (Harbin Institute of Technology), Ministry of Education, Harbin 150090, China*
[2]*School of Civil Engineering, Harbin Institute of Technology, Harbin 150090, China*

Correspondence should be addressed to Huazhang Zhou; huazhang.zhou@hit.edu.cn

Received 4 October 2020; Revised 18 November 2020; Accepted 12 December 2020; Published 28 December 2020

Academic Editor: Min-Juan He

According to the facts of localized crushing failure of bolt groove in wood connection with enough end distance and the three-phase composites of wood with solid (wood substance), water, and gas, a confined compression test for the wood cylinder was conducted for achieving constitutive relation under the complex stress state in wood groove. A porous constitutive model was developed according to the confined compression experiments. Then, the constitutive model was implemented in a finite element modeling of mental dowel-type fasters in wood-to-wood connections to analyse the load-carrying capacity parallel to the grain. Through changing the thicknesses of centre members and side members of wood connections made of a similar wood species, *Pinus Sylvestris* var. *Mongolica*, the effects of thickness combinations of centre members and side members on the failure modes and load-carrying capacity of bolted wood connection including numerical simulations and experiments were compared. The failure modes, including the yielding of centre member, the yielding of side member, and the yielding of the bolt, as well as the rigid rotation of the bolt, all reappeared by the finite element modeling with the porous constitutive model. The predicted deformation shapes and load-displacement relations of bolted wood connections were compared with experimental ones, and good correlations were observed. This paper presents a new approach to simulate the local embedment crushing of bolt groove in wood connections.

1. Introduction

Finite element (FE) numerical simulation of the localized problem in wood structure is always a difficult issue due to the inevitable differences between FE results and experiment results. The reasons causing the differences involve the high variable mechanical properties of wood, differences between clear wood and structural wood, size effect, defects of wood, effect of moisture content, duration of load, and even the test method for material parameters for the localized compression wood. Hence, to reduce the differences between FE simulation and experiment, some hypotheses were adopted in FE modeling to calibrate the mechanical parameters. For example, Moses reduced the initial modulus to cover the work-hardening behaviour of wood, and a multiplier 0.01 was used in the modeling [1]. Guan adopted a modification factor of the empirical modulus to simulate the stiffness of the flat nail embedment test, where a multiplier 0.25 was used [2]. Barrett developed a FE modeling using a foundation material model and limit foundation zone around bolt hole of 4.5 times of diameter of the bolt to simulate the localized problem of nailed connections in wood [3]. Sandhaas developed a continuum damage mechanics model including eight types of failure modes to simulate the performance of timber joints with the slotted-in steel plate, where the size effect for fracture energy was taken into consideration by means of the characteristic element length [4]. By utilizing the modification factors, the simulation results were consistent with those of corresponding experiments. However, the modification factors are always

empirical coefficients which are dependent on the experiences of sophisticated engineers.

Difference induced by the test method for mechanical parameter is also one source for the differences between simulation results and experiment results. The mechanical parameters for the constitutive model in FE modeling were usually determined through uniaxial compression or tension tests. However, in bolted wood connection, the stress state in wood groove is not uniaxial one. Localized wood groove is restrained by lateral wood, which usually deforms along the direction parallel to the grain including shear deformation and crushing deformation components. However, a stress-strain relation from the uniaxial test cannot descript accurately the stress state in wood groove. On the other hand, the dowel-bearing strength test specified in ASTM D5764-97a only specifies the average embedment strength of groove [5]. The embedment strength is also different with the strength from the uniaxial test due to different stress states. Hence, a confined compression test of the wood cylinder was conducted to obtain the real deformation-compression relation in wood groove. A new approach to simulate the localized issue of wood groove in bolted connection by applying the porous constitutive model for wood groove was established to mitigate the dependency on the experiences.

A three-dimensional (3D) FE modeling developed in this paper is based on the phenomena of failure process and failure model of wood groove in bolted connection. During the contacting between bolt and wood groove, localized wood groove is compressed and wood void becomes less and less. If without enough end distance (7d) for the connection, wood groove will crack along the direction of load and shear failure will happen. However, for the connection with enough end distance, only localized wood will be crushed and then plastic hinge may appear in the bolt. In the process of groove crushing, the embedment stiffness of connection changes with the changing of the contact state. At the beginning of contact, embedment stiffness is small. Then, it becomes bigger and nearly keeps a constant. When groove crush is happening, embedment stiffness increases steeply which means that groove becomes compact and the wood void becomes small. In the numerical modeling, the effect of embedment stiffness and strength will be reflected in the porous constitutive by the corresponding relationship between void ratio of wood and pressure on the porous medium.

2. Porous Constitutive Model for Wood

Wood can be seemed as a three-phase medium which is composed of wood solid, liquid, and gas. The wood substance components of wood are the product of wood parenchyma. The liquid component is usually water, and the gas component is usually air. The gaps between the wood substance are called voids. The voids may contain air, water, or both. The void ratio e is the proportion of the volume of voids with respect to the volume of wood substance [6]. Volume of wood changes due to the water expelled from the voids. Mechanical behaviour of wood is also largely dependent on the proportion of wood solids versus voids. When wood is localized compressed, crushing failure is one of typical failure modes and its void ratio becomes less and less. In the elastic stage, the relationship between void ratio and compression stress can be described by a differential equation, the change of the void ratio and the change of logarithm of the equivalent pressure stress [7], shown in the following equation:

$$\mathrm{d}e = -k\,\mathrm{d}\left[\ln\left(p + p_{\mathrm{t}}^{\mathrm{el}}\right)\right], \tag{1}$$

$$p = -\frac{1}{3}\left(\sigma_{\mathrm{R}} + \sigma_{\mathrm{T}} + \sigma_{\mathrm{L}}\right), \tag{2}$$

where e is the void ratio of wood; p is the equivalent pressure stress; σ_{R}, σ_{T}, and σ_{L} are stress components in the directions of radius, tangent, and longitude, respectively; k is the value of the logarithmic bulk modulus, a dimensionless material parameter, which is the slope of the curve between void ratio and the logarithm of the equivalent pressure stress when wood is confined compressed, and it describes the detailed shape of void ratio vs. stress; and $p_{\mathrm{t}}^{\mathrm{el}}$ is the tensile strength of wood.

After using the equivalent pressure stress, the total stress and deviator stress have the following relationships [7]:

$$\begin{aligned} \boldsymbol{\sigma} &= \mathbf{S} - p\mathbf{I}, \\ \mathbf{S} &= 2G\mathbf{e}, \end{aligned} \tag{3}$$

where $\boldsymbol{\sigma}$ is the total stress; $\mathbf{S}$ is the deviator stress; $\mathbf{I}$ is a unit matrix; G is the shear modulus; and $\mathbf{e}$ is the deviator strain [7], which can be expressed as

$$\mathbf{e} = \boldsymbol{\varepsilon} - \frac{1}{3}\varepsilon_{\mathrm{vol}}\mathbf{I}, \tag{4}$$

where $\boldsymbol{\varepsilon}$ is the total strain and $\varepsilon_{\mathrm{vol}}$ is the logarithmic volumetric strain; and $\varepsilon_{\mathrm{vol}} = \ln(\mathrm{d}V/\mathrm{d}V_0)$, where V is the volume of wood and V_0 is the initial volume of wood. Then, the stress and strain can be solved by the above equations.

3. Confined Compression Test of Wood

A setup for the confined compression test was devised to conduct the experiments for obtaining the relationship between void ratio of wood and equivalent pressure in the direction of parallel to grain, shown as in Figure 1(a). A wood cylinder made of the species of *Pinus Sylvestris* var. *mongolica* was inserted into the steel block through a round hole bored in the block. Then, the wood cylinder was compressed by a steel cylinder which was fit to the hole. The diameters of the wood cylinder and the hole are both 20 mm. After sanded by the sand paper, the wood cylinder was inserted in the hole. During the test, the compression velocity of the cylinder was controlled at a rate of 0.5 mm/min [5, 8] and the compression load and displacement were recorded. The information for wood cylinders is shown in Table 1.

Seven wood cylinders with different initial density and different initial void ratio were compressed parallel to grain. Figure 1(b) shows the typical crushing failure mode of the cylinder. The wood cylinders were shortened, and diagonal

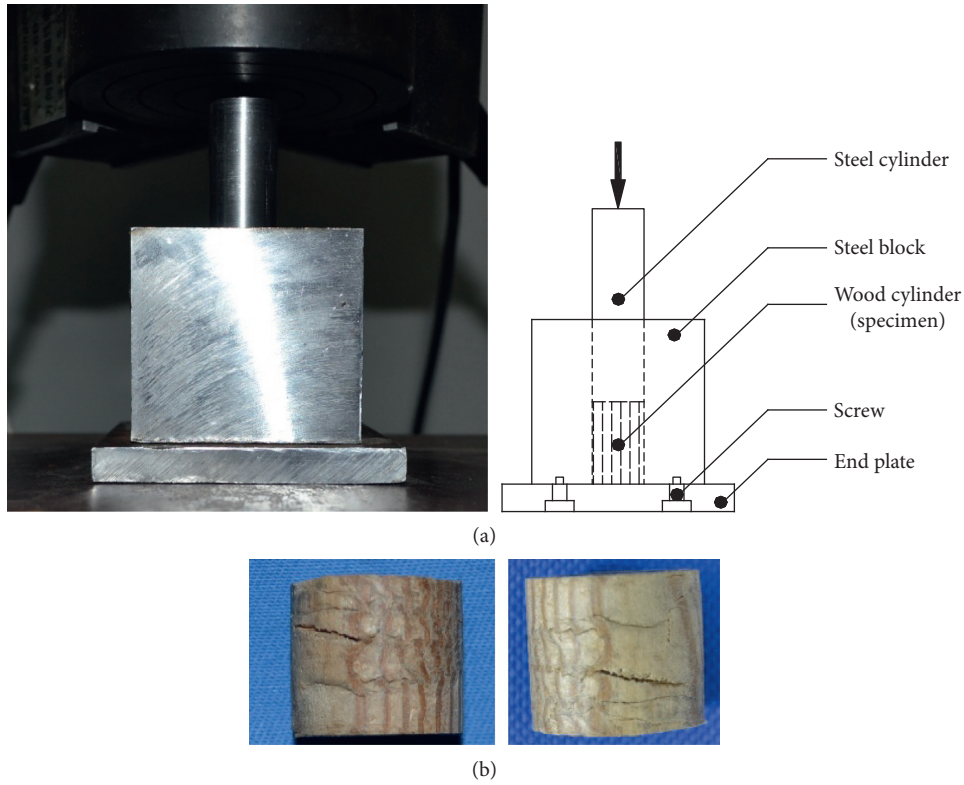

Figure 1: Confined compression test of the wood cylinder parallel to grain: (a) test setup for confined compression experiment; (b) typical crushing failure mode of wood cylinders.

Table 1: The information of wood cylinder specimens for confined compression tests.

Specimen no.	Mass (g)	Initial length (mm)	Initial void ratio
S1	4.317	33.10	3.03
S2	3.863	29.92	2.98
S3	4.638	32.94	2.74
S4	5.272	38.82	2.87
S5	5.768	41.90	2.82
S6	5.459	43.44	3.19
S7	4.188	31.74	2.99

cracks appeared. Figure 2 shows the curves of stress versus elongation parallel to grain from the confined compression tests of wood cylinders.

Based on the relationship among three components including wood substance, water, and void [9], the initial void ratio of wood can be expressed by

$$e_0 = \frac{(1+w)\rho_{wp}}{\rho_0} - 1 = \frac{(1+w)\rho_{wp} S l_0}{m_0} - 1, \quad (5)$$

where e_0, w, and ρ_0 are initial void ratio, moisture content, and density of wood, respectively; ρ_{wp} is the density of the wood solids, for different wood species, $\rho_{wp} = 1.50 - 1.56\,\text{g/cm}^3$, and here an average value [6] was applied; and S, l_0, and m_0 are the cross-section area, initial length, and mass of wood cylinder specimens, respectively. The initial void for wood cylinder specimens is shown in Table 1.

For the confined compression test, the longitudinal strain is not zero, while the tangent strain and radial strain are both zero, which can be derived by the following equation:

$$\begin{bmatrix} \frac{1}{E_L} & -\frac{\nu_{RL}}{E_R} & -\frac{\nu_{TL}}{E_T} \\ -\frac{\nu_{LR}}{E_L} & \frac{1}{E_R} & -\frac{\nu_{TR}}{E_T} \\ -\frac{\nu_{LT}}{E_L} & -\frac{\nu_{RT}}{E_R} & \frac{1}{E_T} \end{bmatrix} \begin{bmatrix} \sigma_L \\ \sigma_R \\ \sigma_T \end{bmatrix} = \begin{bmatrix} \varepsilon_L \\ 0 \\ 0 \end{bmatrix}. \quad (6)$$

Then, the radial stress and tangent stress can be expressed by the longitudinal stress, shown in the following equations:

$$\sigma_R = \frac{\nu_{LR} + \nu_{LT}\nu_{TR}}{1 - \nu_{RT}\nu_{TR}} \frac{E_R}{E_L} \sigma_L, \quad (7)$$

$$\sigma_T = \frac{\nu_{LT} + \nu_{LR}\nu_{RT}}{1 - \nu_{TR}\nu_{RT}} \frac{E_T}{E_L} \sigma_L. \quad (8)$$

For the tested wood species, the elastic ratio and Poisson's ratio [10] are shown in Table 2. After applying the elastic ratio and Poisson's ratio, the equivalent stress of the confined compression wood cylinder can be solved, $\sigma_R = 0.041\sigma_L$, $\sigma_T = 0.031\sigma_L$, and $p = -0.357\sigma_L$, respectively.

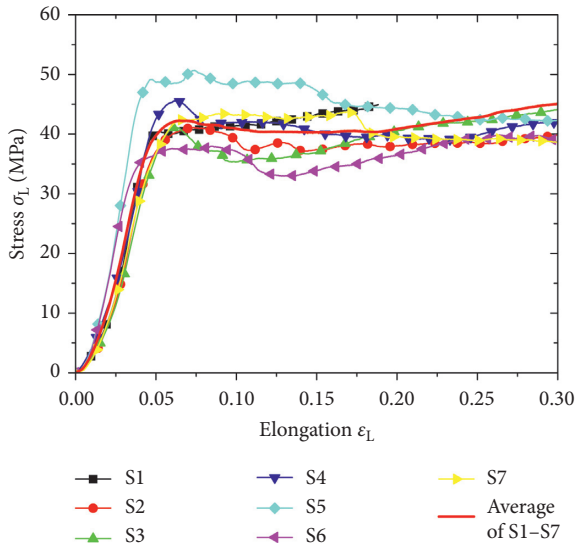

Figure 2: Compression curves of confined compression tests of wood cylinders parallel to the grain.

Table 2: Elastic ratio and Poisson's ratio of wood.

ν_{LR}	ν_{LT}	ν_{RT}	E_T/E_L	E_R/E_L	G_{LR}/E_L	G_{LT}/E_L	G_{RT}/E_L
0.347	0.315	0.408	0.044	0.088	0.096	0.081	0.011

The change of void ratio of the wood cylinder during compressing can be solved by the compression deformation, and its initial void ratio and height can be expressed as

$$\Delta e = e_0 - e = \frac{\Delta h}{h_0}(1 + e_0), \tag{9}$$

where Δe is the change of void ratio of wood, h_0 is the initial length of the wood cylinder, and Δh is the compressive deformation of the wood cylinder. After calculating the equivalent stress p and Δe, curves of the equivalent stress versus the change of void ratio can be obtained, shown as in Figure 3.

Comparing the curves from the experiments of seven wood cylinders in Figure 3(a), the curves of different cylinders with different initial void ratios are close to each other except the specimen S5. However, an average curve of equivalent stress versus change of void ratio can reflect the compression behaviour of wood with the boundary condition of confined restrain. Based on equation (1), the logarithmic bulk modulus of wood was calculated by the average curve. From the average curve shown in Figure 3(b), it can be found that the logarithmic bulk modulus k is not a constant, which reflects three stages of the contact between wood groove and bolt. At the beginning of compression, the logarithmic bulk modulus decreases rapidly until bolt and wood groove contact closely. Then, it nearly keeps a constant. Finally, it climbs rapidly at the same time plasticity is yielded in wood groove. Here, a regressed relationship between the logarithmic bulk modulus k and the change of void ratio Δe was expressed by equation (10) using a polynomial based on the average curve:

$$\begin{aligned} k = {} & 17.910 - 1.279 \times 10^3 \Delta e + 4.116 \times 10^4 \Delta e^2 - 6.850 \times 10^5 \Delta e^3 + 6.343 \times 10^6 \Delta e^4 \\ & - 3.298 \times 10^7 \Delta e^5 + 9.000 \times 10^7 \Delta e^6 - 9.980 \times 10^7 \Delta e^7. \end{aligned} \tag{10}$$

4. FE Modeling and Validation of Embedment Crushing of Wood Groove

4.1. 3D FE Modeling for Bolted Wood Connection. A 3D FE modeling for bolted connection in wood was created using C3D8 solid elements in ABAQUS [7]. Surface contact between wood groove and steel bolt was taken into consideration with the coefficient of friction of 0.15 [11]. The material property of perfect porous elasto-plasticity was assigned to the wood groove zone around the three times of bolt diameter according to crushing deformation in experiment results and FE calculation. A Drucker–Prager plasticity was assigned to wood in the groove zone. The material angle of friction of wood was set as 11°, and dilation angle was zero [4]. An orthotropic elasticity property was assigned to other zones of wood. A perfect elasto-plasticity property was assigned to the steel bolt. The requisite material properties used in FE modeling are listed in Table 3. Here, the properties of clear wood were assigned to the pin groove due to the fact that the wood without defects was usually chosen to make joints and only localized crushing occurred at the joint zone with enough end distance (7d). The dependent relationship of the logarithmic bulk modulus on change of void ratio was implemented in a user defined subroutine UFIELD in which a user defined field variable was defined as the void ratio of each integrate point in the FE software ABAQUS [7].

4.2. Test of Single Bolted Wood Connection. To validate the FE modeling with the perfect elasto-plastic porous constitutive model, 12 lateral resistance tests of single bolt connection of wood made of the species of *Pinus sylvestris* var. *mongolica* were conducted in the direction of parallel to grain according to ASTM D5652 [8]. The dimensions of centre member and side member of connections are all 150 mm in the direction of parallel to grain and 80 mm in the direction of perpendicular to grain, shown as in Figure 4. The diameters of the bolt and groove are 10.5 mm and 13 mm, respectively. The side distance is 40 mm and end distance is 100 mm for every connections. Four groups of thickness combinations for connection specimens, three samples per

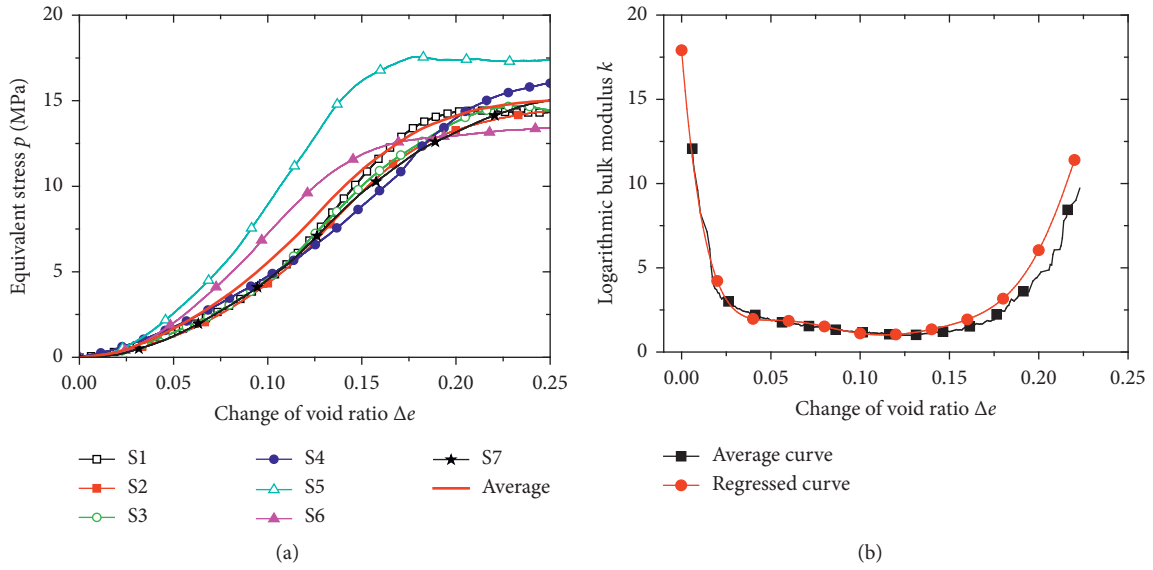

Figure 3: Compression curves of confined compressed wood cylinders parallel to the grain: (a) equivalent stress versus change of void ratio; (b) the logarithmic bulk modulus versus change of void ratio.

Table 3: The material properties for FE modeling.

Requisite constants	Value
Elastic modulus of wood parallel to grain	9000 N/mm^2
Yield stress of wood crushing parallel to grain of wood	40.0 N/mm^2
Tension strength parallel to grain of clear wood	112.9 N/mm^2
Average initial void ratio of wood cylinders	2.944
Elastic modulus of steel bolt	2.06×10^5 N/mm^2
Poisson's ratio of steel bolt	0.3
Yield stress of steel bolt	235 N/mm^2

*The data are from experiments.

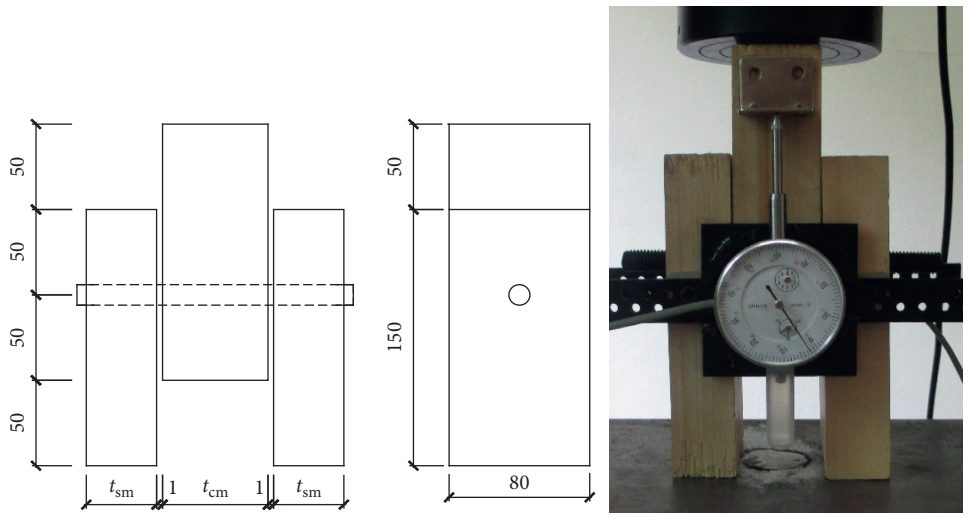

Figure 4: Bolted wood connection.

Table 4: Thickness combinations for bolted wood connections.

	Combination 1	Combination 2	Combination 3	Combination 4
Thickness of centre member, t_{cm} (mm)	40	40	60	60
Thickness of side member, t_{sm} (mm)	30	10	30	60

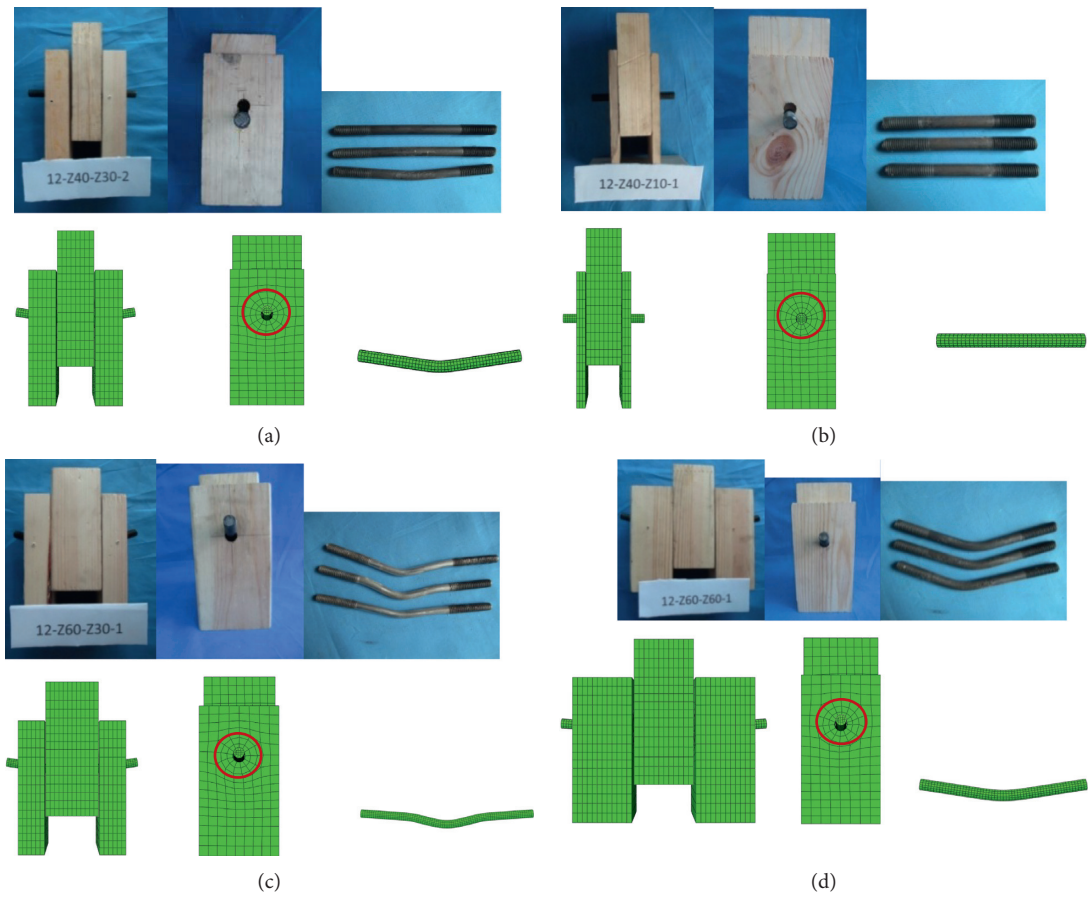

FIGURE 5: Typical failure models of bolt connection with different thickness combinations both in tests and FE simulations: (a) combination 1: $t_{cm} = 40$ mm and $t_{sm} = 30$ mm; (b) combination 2: $t_{cm} = 40$ mm and $t_{sm} = 10$ mm; (c) combination 3: $t_{cm} = 60$ mm and $t_{sm} = 30$ mm; (d) combination 4: $t_{cm} = 60$ mm and $t_{sm} = 60$ mm.

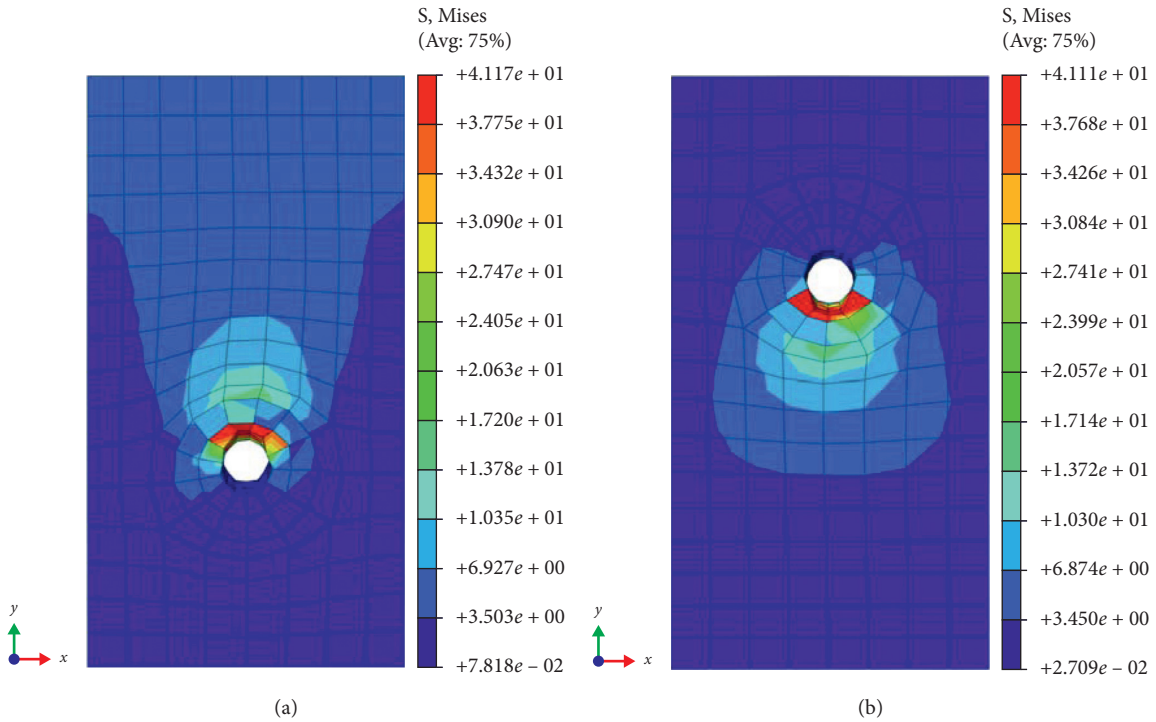

FIGURE 6: Stress contours for wood grooves in (a) centre member and (b) side member (combination 1).

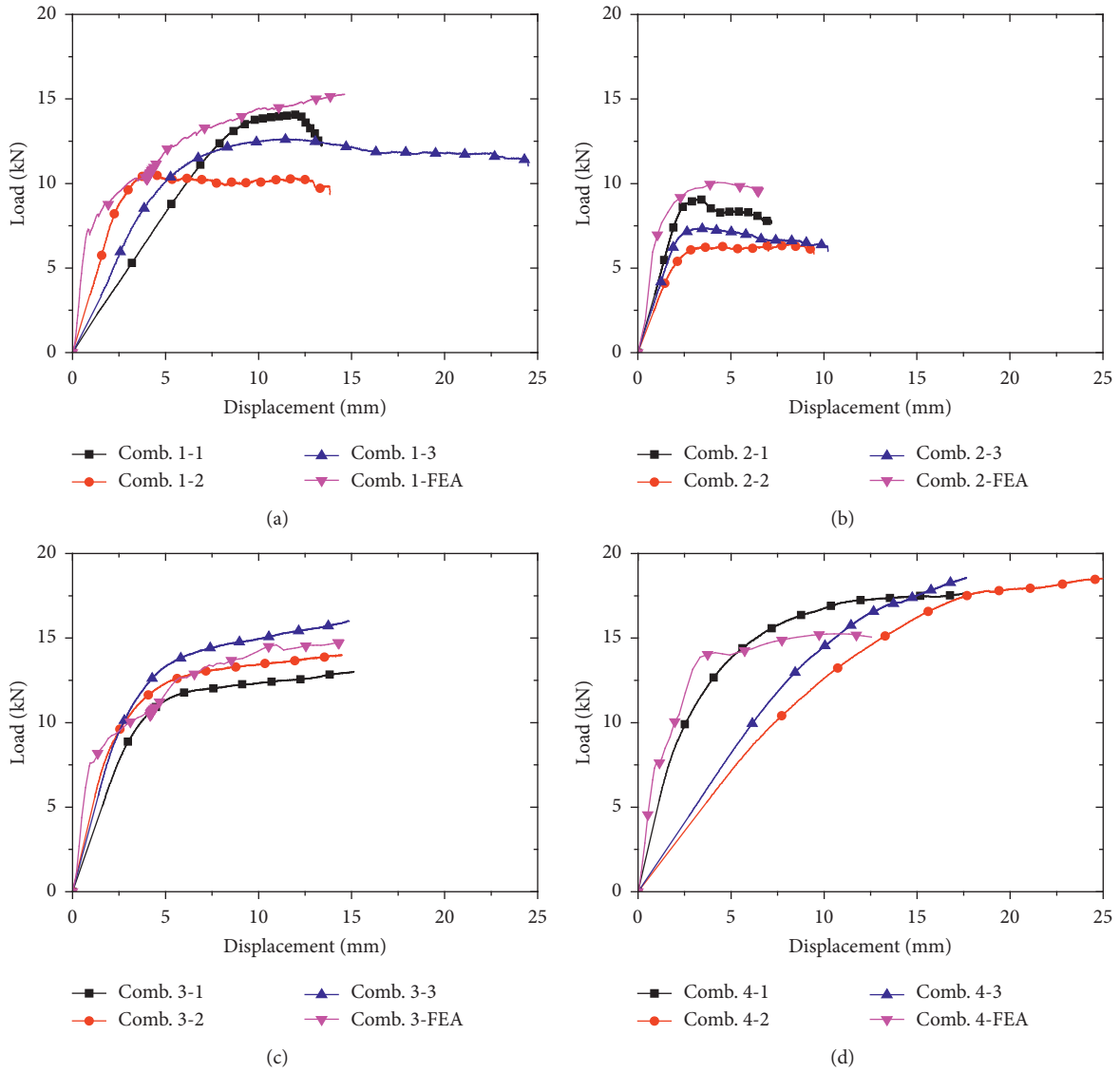

FIGURE 7: The load-displacement curves of single bolt connections: (a) combination 1: $t_{cm} = 40$ mm and $t_{sm} = 30$ mm; (b) combination 2: $t_{cm} = 40$ mm and $t_{sm} = 10$ mm; (c) combination 3: $t_{cm} = 60$ mm and $t_{sm} = 30$ mm; (d) combination 4: $t_{cm} = 60$ mm and $t_{sm} = 60$ mm.

combination, were prepared, whose detail thicknesses are shown in Table 4.

4.3. Validation of FE Modeling. The deformations of all tested connections from different thickness combinations are shown in Figure 5. For each combination, one typical deformed connection and all three deformed bolts are exhibited in the same figure, including these from the tested connection and numerical modeling. The deformation of FE modeling shows good agreement with the experiment observation. Localized crushing failure of pin groove and plastic hinges in the steel bolts appears in different connections. It is obvious that crushing failure did appear at the compressive pin groove, and stress contours for combination 1 are shown in Figure 6. The stress concentration phenomenon and local crushing deformation occur under the contact surface between bolt and groove. The number of plastic hinges in bolts depends on the thickness ratio between the centre member and side member. For the combination 2, the thickness of side member is the thinnest among the four combinations, crushing failure appeared in side member, and the rigid body deformation happened in the bolt. Hence, there was no plastic hinge in the bolt in combination 2. Meanwhile, in combination 4, there were three plastic hinges in the bolt and two hinges in each shear plane. The FE modeling with perfect elasto-plastic porous constitutive exhibits the practicability to simulate the deformation of wood connection including localized deformation of groove and bolt's deformation.

The load-displacement curves for all tested connections and FE simulations are shown in Figure 7. All curves showed the changes of stiffness of bolted connection. The stiffness becomes less and less with the increase in deformation when the localized wood and steel bolt come into plasticity. The

ultimate load from FE results was very close to the maximum loads among three experiment results. While the diameter of the bolt is large and wood members are thin, the yield of groove also can be simulated. The six yield modes for single shear and four yield modes for double shear can all be modeled by the FE modeling. Comparing the deformations of experiments and FE simulations, although the initial stiffness by FE modeling is a little bigger than those of experiments, the overall simulated curves are general accordant with those of experiment curves. The possible reason is that the contact gap between bolt and wood groove brings additional deformation. Hence, the initial stiffness in simulation is more than that of experiment.

5. Conclusions

A method to simulate the localized crushing failure of wood groove in bolted wood connection applying a perfect elastoplasticity porous constitutive model was developed. According to the three-phase composites of wood with solid, water, and gas, wood void ratio expression was derived. A confined compression of the wood cylinder was conducted for void ratio versus stress relationship. The tests can simulate the real stress state in wood groove and provide the FE parameter of wood species for numerical simulation. A relationship between wood void ratio and compression stress was established. The empirical constitutive model for localized crushing wood was validated by the good agreement between experiments and numerical simulations for bolted wood connection with enough end distance (7d). The FE modeling also can predict the load bearing capacity of the all yield modes for single shear and double shear. Its application may be expanded to simulate complex bolted connection in wood structures, such as multiple fastener connections.

Data Availability

The data used to support the findings of this study are available from the corresponding author upon request.

Conflicts of Interest

The authors declare that they have no conflicts of interest.

Acknowledgments

The authors thank the financial support of National Key Research and Development Program of China (no. 2019YFD1101001).

References

[1] D. M. Moses, *Constitutive and analytical models for structural composite lumber with applications to bolted connections*, Ph.D. Dissertation, University of British Columbia, Vancouver, Canada, 2000.

[2] T. Zhou and Z. W. Guan, "A new approach to obtain flat nail embedding strength of double-sided nail plate joints," *Construction and Building Materials*, vol. 25, no. 2, pp. 598–607, 2011.

[3] H. Jung-Pyo and D. Barrett, "Three-dimensional finite-element modelling of nailed connections in wood," *Journal of Structural Engineering*, vol. 136, no. 6, pp. 715–722, 2010.

[4] S. Carmen, *Mechanical behaviour of timber joints with slotted-in steel plates*, Ph.D. Dissertation, Technology University Delft, Delfts, Netherlands, 2012.

[5] ASTM D 5764-97a, *Standard Test Method for Evaluating Dowel-Bearing Strength of Wood and Wood-Based Products*, American Society for Testing and Materials, West Conshohocken, PA, USA, 2002.

[6] F. F. P. Kollmann, A. Wilfred, and J. R. Cote, *Principles of Wood Science and Technology, 1 Solid Wood*, Springer-Verlag New Yourk Inc, New York, NY, USA, 1968.

[7] D. S. Simulia, *ABAQUS 6.14. ABAQUS Theory Guide*, Dassault Systèmes Simulia Corp., Johnston, RI, USA, 2014.

[8] ASTM D 5652-95, *Standard Test Methods for Bolted Connections in Wood and Wood–Based Products*, American Society for Testing and Materials, West Conshohocken, PA, USA, 2002.

[9] M. D. Wood, *Soil Behaviour and Critical State Soil Mechanics*, Cambridge University Press, Cambridge, UK, 1990.

[10] D. W. Green, E. Winandy Jerrold, and E. Kretschmann David, *Mechanical Properties of Wood, Wood as an Engineering Material*, Forest Products Laboratory, Madison, WI, USA, 1999.

[11] W. Simpson and T. W. Anton, *Physical Properties and Moisture Relations of Wood: Wood Handbook, Wood as an Engineering Material*, Forest Products Laboratory, Madison, WI, USA, 1999.